JACS
JOURNAL OF THE AMERICAN CHEMICAL SOCIETY

Communication

pubs.acs.org/JACS

A Redox Responsive, Fluorescent Supramolecular Metallohydrogel Consists of Nanofibers with Single-Molecule Width

Ye Zhang,[†] Bei Zhang,[‡] Yi Kuang,[†] Yuan Gao,[†] Junfeng Shi,[†] Xi Xiang Zhang,[‡] and Bing Xu*[,†]

[†]Department of Chemistry, Brandeis University, 415 South Street, Waltham, Massachusetts 02454, United States

[‡]Advanced Nano-fabrication, Imaging and Characterization Core Lab, King Abdullah University of Science and Technology, Thuwal 23955-6900, Saudi Arabia

Supporting Information

ABSTRACT: The integration of a tripeptide derivative, which is a versatile self-assembly motif, with a ruthenium(II)tris(bipyridine) complex affords the first supramolecular metallo-hydrogelator that not only self assembles in water to form a hydrogel but also exhibits gel−sol transition upon oxidation of the metal center. Surprisingly, the incorporation of the metal complex in the hydrogelator results in the nanofibers, formed by the self-assembly of the hydrogelator in water, to have the width of a single molecule of the hydrogelator. These results illustrate that metal complexes, besides being able to impart rich optical, electronic, redox, or magnetic properties to supramolecular hydrogels, also offer a unique geometrical control to prearrange the self-assembly motif prior to self-assembling. The use of metal complexes to modulate the dimensionality of intermolecular interactions may also help elucidate the interactions of the molecular nanofibers with other molecules, thus facilitating the development of supramolecular hydrogel materials for a wide range of applications.

This communication reports the incorporation of a metal complex in a hydrogelator for the development a redox responsive, fluorescent supramolecular hydrogel consisting of nanofibers resulting from one-dimensional (1D) intermolecular interactions. As the result of molecular self-assembly[1] driven by multiple noncovalent interactions in water, supramolecular hydrogels[2,3] formed by small molecules[4] have received considerable attentions recently because they promise soft materials with various important applications in biomedicines, such as drug delivery,[5,6] cell culture,[7] and sensors.[8] These supramolecular hydrogelators are usually organic molecules,[2] and a large portion of them are peptides or peptide derivatives.[9] Unlike the case of hydrogels, it is relatively common to utilize metal complexes as organogelators in the development of organgels[10] due to their rich optical, electronic, redox, or magnetic properties usually associated with metal centers and the stability of metal complexes in common organic solvents. For example, metal complex-based organogelators have exhibited a wide range of interesting properties, such as anion binding,[11] fluorescence,[12] color switch,[13] catalysis,[14] and responses to ultrasound,[15] redox perturbation,[16] or temperature.[17] Encouraged by these successful developments of organogelators made of metal complexes, we chose to develop hydrogelators containing metal complexes and refer to this type of hydrogelator as metallo-hydrogelators, which is a type of rarely explored building blocks of supramolecular hydrogels[18] despite the aforementioned properties of metal complexes.

In this work, we chose the ruthenium(II)tris(bipyridine) $[Ru(bipy)_3]^{2+}$ derivative as the metal complex for making metallo-hydrogelators because of its octahedral geometry and rich functions (e.g., as photocatalysts, as building blocks for conducting polymers, as DNA probes, or as fluorophores for electrochemoluminescence).[19] Although $[Ru(bipy)_3]^{2+}$ has served as the components for organogelators,[20] it has yet to be integrated with peptides to form supramolecular hydrogels. Thus, we designed and synthesized a ruthenium(II)tris(bipyridine) complex (**3**) that bears a molecular motif (**1**) known to promote self-assembly in water.[6] While the ligand (**2**) itself fails to form a supramolecular hydrogel, the complex (**3**) acts as a metallo-hydrogelator that forms nanofibers at an exceptionally low critical concentration (0.00625% (w/v)) and supramolecular hydrogels over a wide pH range (pH 1−10). Being excited at 470 nm, the hydrogels of **3** exhibit an intense fluorescence with a maximum at 630 nm. Upon oxidation of the ruthenium from Ru(II) to Ru(III), the nanofibers of **3** break down to turn the hydrogel into a solution, accompanied by a significant decrease of the circular dichroism (CD) signal. Most intriguingly, high-resolution transmission electron microscopy (HRTEM) indicates that the self-assembly of **3** results in the nanofibers of **3** to have the width of a single molecule of **3**. This result suggests that the geometry associated with $[Ru(bipy)_3]^{2+}$ favors one-dimensional (1D) intermolecular interactions of **3**, thus limiting the width of the supramolecular nanofibers of **3**. This subtle, yet previously unknown observation related to metal complexes, may lead to a facile approach for designing a new type of supramolecular nanofibers based on the geometries (e.g., octahedral, square planar, etc.) of metal complexes, which usually are unattainable by simple organic molecules alone. In addition, being more biocompatible than common polypyridyl ruthenium complex,[21] **3** also promises applications in molecular imaging.[22]

Scheme 1 shows the chemical structures of the molecular motif (**1**) known to self assemble in water,[6] the ligand (**2**) consisting of a bipyridine and **1**, and the metallo-hydrogelator (**3**). After being obtained through solid-phase synthesis according to the reported procedure,[6] **1** reacts with 4,4′-

Received: March 10, 2013
Published: March 25, 2013

   dx.doi.org/10.1021/ja402490j | J. Am. Chem. Soc. 2013, 135, 5008−5011

Scheme 1. Molecular Structures and CPK Models of the Self-Assembly Motif, the Ligand, and the Metallo-Hydrogelator

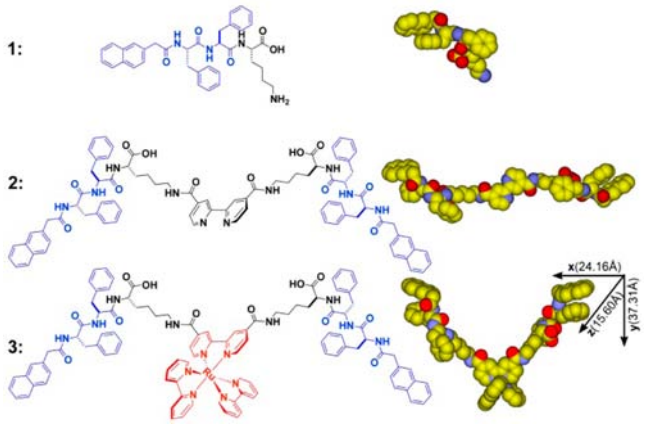

dicarboxyl-2,2′-bipyridine[23] to afford the ligand (**2**) in 56% yield (Scheme S1 in Supporting Information [SI]). However, **2** is unable to form a supramolecular hydrogel upon changing pH or temperature. The aggregation of **2** only results in some precipitates, suggesting strong intermolecular interactions among the molecules of **2**. The organic functional groups (i.e., carboxylates or amides) appear to prevent **2** from reacting directly with a known polypyridyl ruthenium complex, $[Ru(bipy)2]Cl_2$,[24] for making **3**. Thus, we used Ru(II)-$(bipy)_2$(4,4′-dicarboxyl-2,2′-bipyridine)dichloride to react with **1** to form **3** in moderate yield (Scheme S2 in SI). **3** is able to form hydrogels over a wide range of pH at various concentrations. For example, at pH = 1, it forms a soft gel at a concentration of 0.1% (w/v) and a firm gel at a concentration of 0.4% (w/v) (Figure S1 in SI). At pH = 7, it forms a soft gel at a concentration of 0.2% (w/v) and a firm gel at a concentration of 0.8% (w/v) (Figure 1A, Figure S2 in SI).

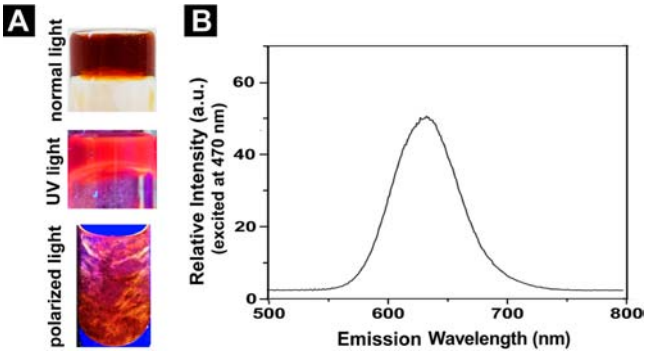

Figure 1. (A) Optical images of hydrogel formed by **3** (0.8% w/v) in water at pH = 7 under normal light, UV (long wavelength) light, and polarized light. (B) Emission (excited at 470 nm) spectrum of the hydrogel in (A).

These results agree with that of the protonation of the carboxyl groups on **3**, where low pH decreases the solubility of **3** and thus favors the formation of hydrogels. Being consistent with the well-known photochemical properties of $[Ru(bipy)_3]^{2+}$, the hydrogel of **3** exhibits strong fluorescence upon the irradiation of UV light (Figure 1A). According to its absorbance (Figure S8 in SI) and fluorescent spectrum (Figure 1B), the hydrogel of **3**, being excited at 470 nm, fluoresces with the emission maximum at 630 nm. Being placed between a pair of crossed polarizers, the hydrogel of **3** also shows birefringence (Figure 1A). Because the hydrogel of **1** lacks this interesting property, the anisotropy of the hydrogel of **3** likely relates to the incorporation of $[Ru(bipy)_3]^{2+}$ in **3**.

Hydrogelator **3** preserves the redox property of a polypyridyl ruthenium complex. Using $Ce(SO_4)_2$ to oxidize the hydrogel of **3**, we obtain a yellow emulsion during the process, and it eventually turns into a transparent solution (Figure 2A) that is

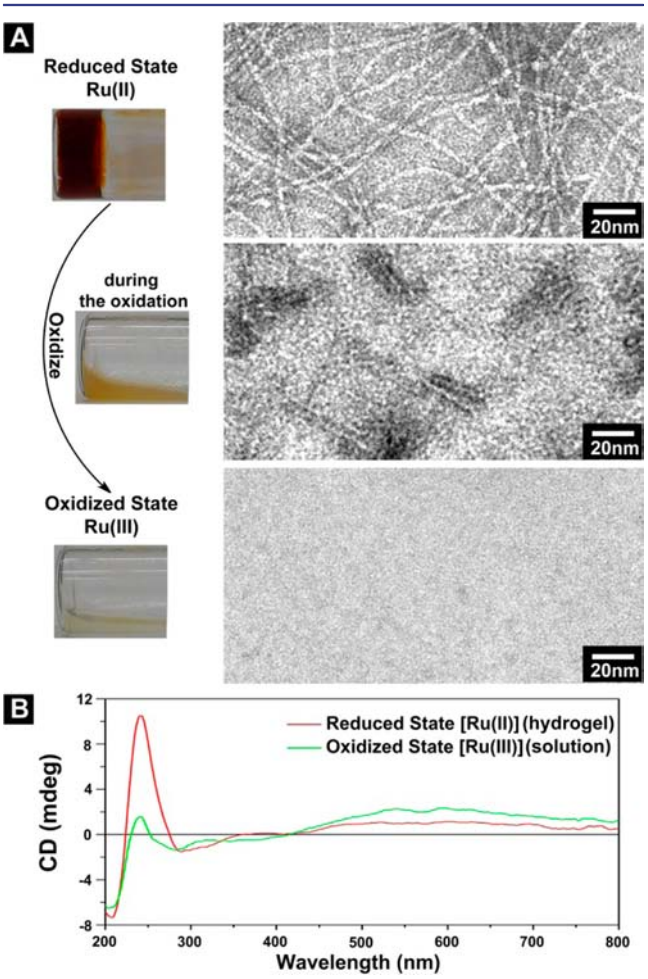

Figure 2. (A) Optical images of oxidation-induced gel−sol transition and the TEM images corresponding to the samples at different states of transition. The hydrogel (reduced state) is formed by 0.8% (w/v) **3** in water at pH = 1. Scale bar is 10 nm. (B) CD spectrum of the hydrogel (reduced state) and the solution (oxidized state).

not fluorescent (Figure S5 in SI). Figure 2A shows the HRTEM images of the samples at different stages of oxidation carried out at acidic conditions (pH 1). At the reduced state (Ru(II)), the hydrogel of **3** consists of long and relatively flexible nanofibers that have the diameter of about 3 nm and entangle with each other to form a network. When the hydrogel becomes a yellow emulsion during oxidation, TEM reveals that the network of the nanofibers breaks apart and only scattered short nanofibers (about 3 nm in diameter and less than 30 nm in length) exist. When the emulsion becomes transparent at the final stage of oxidation, TEM of the solution gives hardly any features, suggesting that the nanofibers of **3** dissociate completely upon oxidation. According to Figure 2B, the CD spectra also agree with the dissociation of the nanofibers of **3** caused by oxidation. Particularly, the significant decrease of the

dx.doi.org/10.1021/ja402490j | J. Am. Chem. Soc. 2013, 135, 5008−5011

CD signals of the far UV region (185−260 nm), due to gel−sol transition, indicate that the secondary structures resulting from the peptide motif of **3** in the gel phase largely dissociate in the solution phase, resulting from the oxidation of **3**. Little change of the CD signals originates from naphthalene in the near-UV region (260−350 nm), and the slight increase of the CD signals originating from metal-to-ligand charge transfer (MLCT) (>450 nm) imply that the chiral center on the peptides induces these CD signals (ICD),[25] which are less sensitive to the loss of the secondary structures. These results indicate that the redox change of the metal center of **3** induced the transition of the self-assembled structure of **3** in water.

HRTEM images of the hydrogel of **3** (Figure 3A) reveal an unexpected result that the diameters of the nanofibers of **3** (3.1 ± 0.1 nm) are narrower than those of the hydrogel of **1** (5.8 ± 0.1 nm, Figure S7 in SI) even though **1** has a much smaller molecular size (Figure S12 in SI) than **3** does. To understand the superstructure of the nanofibers formed by self-assembly of **3**, we evaluated the conformations and the molecular dimension of **3**. According to the minimized conformation calculated by molecular mechanics (MM), **3** has a dimension of 37.3 Å × 24.2 Å × 15.6 Å (Scheme 1), which suggests that the nanofibers in the hydrogel of **3** have the width of a single molecule of **3**. Figure 3B shows a plausible model of the nanofibers of **3**, in which the intermolecular aromatic−aromatic interactions from the overlapping of phenyl and/or naphthyl groups between **3** result in the supramolecular chains (Figure 3C). These 1D intermolecular interactions favor the formation of nanofibers at the exceptional low concentration of **3** (0.00625% (w/v), Figure S3 in SI) before **3** reaches the minimum gelation concentration (0.1% (w/v)) at pH = 1 (Figure S1 in SI). TEM images (Figure S4 in SI) also indicate that **3** self assembles to form nanofibers at the minimum concentration of 0.1% (w/v) and pH of 7. There is little difference among the nanofibers formed by **3** in water even when they are formed under different conditions (Figure S4 in SI). This observation agrees with the 1D model (Figure 3B). In addition to the octahedral geometry that may disfavor the packing of the molecular nanofibers to form bundles, the charge repulsion between the ruthenium complexes also likely contributes to the separation of the molecular nanofibers. Except for two pairs of intramolecular hydrogen bonds formed by amide groups and hydroxyl groups of **3**, the remaining amide groups and hydroxyl groups would be available for forming hydrogen bonds with water molecules (Figure 3C). These interactions allow the supramolecular chains, even at a relatively low molecular density, to hold a considerable amount of water, which results in a hydrogel at a rather low minimal gelation concentration of **3**. Moreover, this kind of 1D intermolecular interaction resulting from the motif of **1** also contributes to a similar trend where there are slightly lower storage moduli of the hydrogel of **3** than those of the hydrogel of **1** at the same concentration and at pH = 7 (Figure S9 in SI).

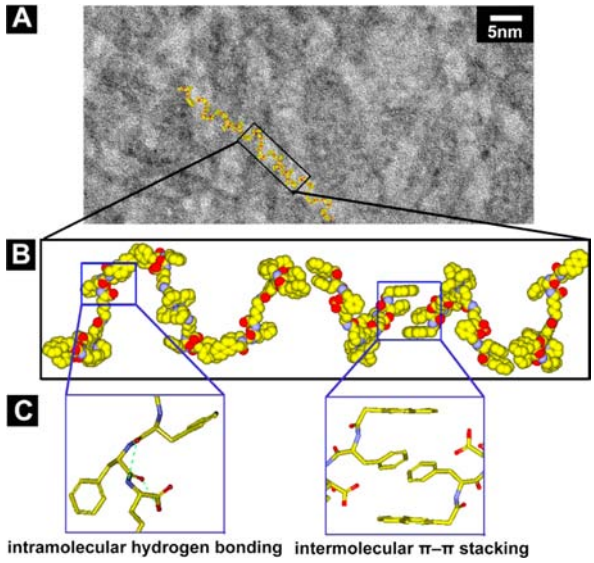

Figure 3. (A) High-resolution TEM (HRTEM) image (scale bar is 5 nm) of the nanofibers in hydrogel of **3** (0.4% (w/v), pH = 1). (B) According to the TEM, a tentative molecular arrangement in the nanofibers of **3**. (C) Illustrations of plausible intramolecular hydrogen bonds (green dashed line) and intermolecular $\pi-\pi$ stacking.

In conclusion, this work, as the first example of ruthenium complex-based supramolecular hydrogelators, illustrates a useful approach that incorporates functional metal complexes into peptide-based hydrogelators for the development of a multifunctional self-assembly system and materials. Although the molecular model of the nanofibers of **3** is tentative, the single-molecule width of the nanofibers should be beneficial for studying the interaction of the supramolecular nanofibers with other molecules/targets. Interestingly, **3**, consisting of the tripeptide motifs, exhibits little affinity to nucleic acids (Figure S10 in SI) thus becoming cell compatible at a relatively high concentration (Figure S11 in SI). This feature, which agrees well with the origin of the cytotoxicity of polypyridyl ruthenium complex,[21] may allow **3** to serve as a multipurpose hydrogelator and find application in live-cell imaging (Figure 4). In fact, TEM reveals that the molecules of **3** are able to form nanofibers (Figure S6 in SI) at 200 μM in cell culture medium, suggesting that the nanofibers of **3** also enter the cells. Moreover, we envision that, with future advances of fluorescent imaging techniques, the long fluorescence lifetime of $[Ru(bipy)_3]^{2+}$ derivative[26] may allow the use of nanofibers of **3** of single-molecule width to elucidate the interaction between these supramolecular nanofibers with proteins in live cells.

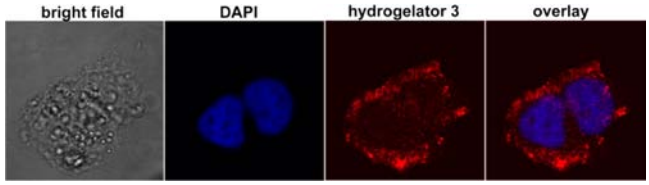

Figure 4. Fluorescent image of a HeLa cell incubated with **3** (200 μM, 24 h). From left to right: phase-contrast image, live cell stain DAPI (blue), luminescence emission of **3** (red), and overlay image.

■ ASSOCIATED CONTENT

Ⓢ Supporting Information

Synthetic procedures and characterization methods, Schemes S1 and S2, and Figures S1−S12. This material is available free of charge via the Internet at http://pubs.acs.org.

■ AUTHOR INFORMATION

Corresponding Author

bxu@brandeis.edu

Notes

The authors declare no competing financial interest.

■ ACKNOWLEDGMENTS

This work was partially supported by a grant from the Army Research Office (ARO 56735-MS), a National Science Foundation MRSEC Grant (DMR-0820492), NIH (R01 CA142746), and start-up funds from Brandeis University. The TEM images were taken at the EM facility of Brandeis University.

■ REFERENCES

(1) (a) Lehn, J. M. *Angew. Chem., Int. Ed.* **1990**, *29*, 1304. (b) Whitesides, G. M.; Mathias, J. P.; Seto, C. T. *Science* **1991**, *254*, 1312. (c) Hasenknopf, B.; Lehn, J. M.; Boumediene, N.; DupontGervais, A.; VanDorsselaer, A.; Kneisel, B.; Fenske, D. *J. Am. Chem. Soc.* **1997**, *119*, 10956. (d) Whitesides, G. M.; Grzybowski, B. *Science* **2002**, *295*, 2418.

(2) Estroff, L. A.; Hamilton, A. D. *Chem. Rev.* **2004**, *104*, 1201.

(3) (a) Yang, Z.; Liang, G.; Xu, B. *Acc. Chem. Res.* **2008**, *41*, 315. (b) Zhang, Y.; Gu, H. W.; Yang, Z. M.; Xu, B. *J. Am. Chem. Soc.* **2003**, *125*, 13680. (c) Toledano, S.; Williams, R. J.; Jayawarna, V.; Ulijn, R. V. *J. Am. Chem. Soc.* **2006**, *128*, 1070. (d) Nagarkar, R. P.; Hule, R. A.; Pochan, D. J.; Schneider, J. P. *J. Am. Chem. Soc.* **2008**, *130*, 4466. (e) Bowerman, C. J.; Nilsson, B. L. *J. Am. Chem. Soc.* **2010**, *132*, 9526.

(4) (a) Li, X. M.; Kuang, Y.; Shi, J. F.; Gao, Y.; Lin, H. C.; Xu, B. *J. Am. Chem. Soc.* **2011**, *133*, 17513. (b) Mukhopadhyay, S.; Maitra, U.; Ira; Krishnamoorthy, G.; Schmidt, J.; Talmon, Y. *J. Am. Chem. Soc.* **2004**, *126*, 15905. (c) Vemula, P. K.; Li, J.; John, G. *J. Am. Chem. Soc.* **2006**, *128*, 8932. (d) Appel, E. A.; Biedermann, F.; Rauwald, U.; Jones, S. T.; Zayed, J. M.; Scherman, O. A. *J. Am. Chem. Soc.* **2010**, *132*, 14251. (e) Johnson, E. K.; Adams, D. J.; Cameron, P. J. *J. Am. Chem. Soc.* **2010**, *132*, 5130. (f) Channon, K. J.; Devlin, G. L.; Magennis, S. W.; Finlayson, C. E.; Tickler, A. K.; Silva, C.; MacPhee, C. E. *J. Am. Chem. Soc.* **2008**, *130*, 5487.

(5) (a) Pouget, E.; Fay, N.; Dujardin, E.; Jamin, N.; Berthault, P.; Perrin, L.; Pandit, A.; Rose, T.; Valery, C.; Thomas, D.; Paternostre, M.; Artzner, F. *J. Am. Chem. Soc.* **2010**, *132*, 4230. (b) Boekhoven, J.; Koot, M.; Wezendonk, T. A.; Eelkema, R.; van Esch, J. H. *J. Am. Chem. Soc.* **2012**, *134*, 12908. (c) Cheetham, A. G.; Zhang, P.; Lin, Y.-a.; Lock, L. L.; Cui, H. *J. Am. Chem. Soc.* **2013**, *135*, 2907. (d) Li, J. Y.; Kuang, Y.; Gao, Y.; Du, X. W.; Shi, J. F.; Xu, B. *J. Am. Chem. Soc.* **2013**, *135*, 542.

(6) Gao, Y.; Kuang, Y.; Guo, Z. F.; Guo, Z. H.; Krauss, I. J.; Xu, B. *J. Am. Chem. Soc.* **2009**, *131*, 13576.

(7) (a) Kisiday, J.; Jin, M.; Kurz, B.; Hung, H.; Semino, C.; Zhang, S.; Grodzinsky, A. J. *Proc. Natl. Acad. Sci. U.S.A.* **2002**, *99*, 9996. (b) Silva, G. A.; Czeisler, C.; Niece, K. L.; Beniash, E.; Harrington, D. A.; Kessler, J. A.; Stupp, S. I. *Science* **2004**, *303*, 1352. (c) Li, X. M.; Kuang, Y.; Lin, H. C.; Gao, Y.; Shi, J. F.; Xu, B. *Angew. Chem., Int. Ed.* **2011**, *50*, 9365. (d) Zhou, M.; Smith, A. M.; Das, A. K.; Hodson, N. W.; Collins, R. F.; Ulijn, R. V.; Gough, J. E. *Biomaterials* **2009**, *30*, 2523.

(8) (a) Wada, A.; Tamaru, S.; Ikeda, M.; Hamachi, I. *J. Am. Chem. Soc.* **2009**, *131*, 5321. (b) Kiyonaka, S.; Sada, K.; Yoshimura, I.; Shinkai, S.; Kato, N.; Hamachi, I. *Nat. Mater.* **2004**, *3*, 58. (c) Chen, J.; McNeil, A. J. *J. Am. Chem. Soc.* **2008**, *130*, 16496. Gao, Y.; Shi, J. F.; Yuan, D.; Xu, B. 2012, *3*, 1033. Chen, S. J.; Chen, L. J.; Yang, H. B.; Tian, H.; Zhu, W. H. *J. Am. Chem. Soc.* **2012**, *134*, 13596.

(9) Cui, H. G.; Webber, M. J.; Stupp, S. I. *Biopolymers* **2010**, *94*, 1.

(10) (a) Terech, P.; Weiss, R. G. *Chem. Rev.* **1997**, *97*, 3133. (b) van Esch, J. H.; Feringa, B. L. *Angew. Chem., Int. Ed.* **2000**, *39*, 2263.

(11) (a) Lloyd, G. O.; Steed, J. W. *Nat. Chem.* **2009**, *1*, 437. (b) Piepenbrock, M. O. M.; Clarke, N.; Steed, J. W. *Langmuir* **2009**, *25*, 8451.

(12) (a) Tam, A. Y. Y.; Wong, K. M. C.; Yam, V. W. W. *J. Am. Chem. Soc.* **2009**, *131*, 6253. (b) Lu, W.; Law, Y. C.; Han, J.; Chui, S. S. Y.; Ma, D. L.; Zhu, N. Y.; Che, C. M. *Chem.—Asian J.* **2008**, *3*, 59.

(13) Kishimura, A.; Yamashita, T.; Aida, T. *J. Am. Chem. Soc.* **2005**, *127*, 179.

(14) Xing, B. G.; Choi, M. F.; Xu, B. *Chem.—Eur. J.* **2002**, *8*, 5028.

(15) (a) Zhang, S. Y.; Yang, S. J.; Lan, J. B.; Tang, Y. R.; Xue, Y.; You, J. S. *J. Am. Chem. Soc.* **2009**, *131*, 1689. (b) Paulusse, J. M. J.; van Beek, D. J. M.; Sijbesma, R. P. *J. Am. Chem. Soc.* **2007**, *129*, 2392.

(16) Gasnier, A.; Royal, G.; Terech, P. *Langmuir* **2009**, *25*, 8751.

(17) Kuroiwa, K.; Shibata, T.; Takada, A.; Nemoto, N.; Kimizuka, N. *J. Am. Chem. Soc.* **2004**, *126*, 2016.

(18) (a) Wang, J.; Chen, Y.; Law, Y. C.; Li, M. Y.; Zhu, M. X.; Lu, W.; (b) Chui, S. S. Y.; Zhu, N. Y.; Che, C. M. *Chem.—Asian J.* **2011**, *6*, 3011. (c) Pan, Y.; Gao, Y.; Shi, J. F.; Wang, L.; Xu, B. *J. Mater. Chem.* **2011**, *21*, 6804. (d) Joshi, S. A.; Kulkarni, N. D. *Chem. Commun.* **2009**, 2341.

(19) (a) Zhu, S. S.; Swager, T. M. *Adv. Mater.* **1996**, *8*, 497. (b) Kaes, C.; Katz, A.; Hosseini, M. W. *Chem. Rev.* **2000**, *100*, 3553.

(20) Suzuki, M.; Waraksa, C. C.; Mallouk, T. E.; Nakayama, H.; Hanabusa, K. *J. Phys. Chem. B* **2002**, *106*, 4227.

(21) (a) Novakova, O.; Kasparkova, J.; Vrana, O.; Vanvliet, P. M.; Reedijk, J.; Brabec, V. *Biochemistry* **1995**, *34*, 12369. (b) Pierroz, V.; Joshi, T.; Leonidova, A.; Mari, C.; Schur, J.; Ott, I.; Spiccia, L.; Ferrari, S.; Gasser, G. *J. Am. Chem. Soc.* **2012**, *134*, 20376.

(22) (a) Gao, W. Z.; Xing, B. G.; Tsien, R. Y.; Rao, J. H. *J. Am. Chem. Soc.* **2003**, *125*, 11146. (b) So, M. K.; Xu, C. J.; Loening, A. M.; Gambhir, S. S.; Rao, J. H. *Nat. Biotechnol.* **2006**, *24*, 339.

(23) Maerker, G.; Case, F. H. *J. Am. Chem. Soc.* **1958**, *80*, 2745.

(24) (a) Anderson, S.; Constable, E. C.; Seddon, K. R.; Turp, J. E.; Baggott, J. E.; Pilling, M. J. *J. Chem. Soc., Dalton Trans.* **1985**, 2247. (b) Schwalbe, M.; Schafer, B.; Gorls, H.; Rau, S.; Tschierlei, S.; Schmitt, M.; Popp, J.; Vaughan, G.; Henry, W.; Vos, J. G. *Eur. J. Inorg. Chem.* **2008**, 3310. (c) Sun, Y. L.; Machala, M. L.; Castellano, F. N. *Inorg. Chim. Acta* **2010**, *363*, 283.

(25) Shiraki, T.; Dawn, A.; Tsuchiya, Y.; Shinkai, S. *J. Am. Chem. Soc.* **2010**, *132*, 13928.

(26) Yoshimizu, H.; Asakura, T.; Kaneko, M. *Macromol. Chem. Phys.* **1991**, *192*, 1649.